

Angular distributions of the alpha particle production in the ${}^7\text{Li}+{}^{144}\text{Sm}$ system at near-barrier energies

This content has been downloaded from IOPscience. Please scroll down to see the full text.

2015 J. Phys.: Conf. Ser. 630 012023

(<http://iopscience.iop.org/1742-6596/630/1/012023>)

View [the table of contents for this issue](#), or go to the [journal homepage](#) for more

Download details:

IP Address: 200.82.123.175

This content was downloaded on 30/04/2016 at 21:49

Please note that [terms and conditions apply](#).

Angular distributions of the alpha particle production in the ${}^7\text{Li}+{}^{144}\text{Sm}$ system at near-barrier energies

P F F Carnelli^{1,2,3}, A Arazi^{1,3}, O A Capurro¹, J O Fernández Niello^{1,2,3}, D Martínez Heimann^{1,2,3}, A J Pacheco^{1,3}, M A Cardona^{1,3}, E de Barbará¹, J M Figueira^{1,3}, D L Hojman^{1,3}, G V Martí¹ and A E Negri^{1,2,3}

¹ Laboratorio TANDAR, Comisión Nacional de Energía Atómica, Av. Gral. Paz 1499, B1650KNA San Martín, Buenos Aires, Argentina

² Instituto de Investigación e Ingeniería Ambiental, Universidad Nacional de San Martín, 25 de Mayo y Francia, B1650BWA San Martín, Buenos Aires, Argentina

³ Consejo Nacional de Investigaciones Científicas y Técnicas, Av. Rivadavia 1917, C1033AAJ Buenos Aires, Argentina

E-mail: pcarnelli@unsam.edu.ar

Abstract. We have studied the production of alpha particles in reactions induced by ${}^7\text{Li}$ projectiles on a ${}^{144}\text{Sm}$ target at bombarding energies of 18, 24 and 30 MeV over the 15° - 140° angular range. The purpose of the investigation has been to determine the contribution of different mechanisms in reactions that involve weakly bound projectiles. We have included in our analysis several processes that can either directly or sequentially lead to the emission of alpha particles: complete fusion, direct transfer of ${}^3\text{H}$, capture breakup (incomplete fusion, sequential complete fusion) and non-capture breakup. In order to distinguish alpha particles stemming from these processes it is necessary to determine the mass and charge of the reaction products and to obtain precise measurements of their energies and scattering angles over relatively wide ranges of these variables. We have done this using a detection system consisting of an ionization chamber plus three position sensitive detectors. We present results of these measurements and a preliminary interpretation based on kinematical considerations and comparisons with predictions from a statistical model.

1. Introduction

The influence of breakup on other reaction channels (such as elastic scattering and fusion) in systems involving weakly bound projectiles at energies around the Coulomb barrier has been an extensively studied subject over the last several years (see Ref. [1] and references therein). Due to the small separation energies involved, breakup reactions are known to account in these cases for a significant part of the total cross section and in particular, weakly bound stable nuclei are a useful alternative to investigate the various aspects of this kind of processes. It is known, or it has been postulated, that the breakup of the projectile may have several outcomes: *i*) all the fragments may scatter away (non-capture breakup), *ii*) one of the fragments may be captured by the target whereas the other scatters away (incomplete fusion), or *iii*) all breakup fragments may be captured by the target (complete fusion following breakup). Even more complex processes, such as transfer reactions followed by the breakup of the remaining (projectile-like) nucleus, have also been observed. For example, for the ${}^7\text{Li}$ projectile, the above mentioned mechanism could consist in either neutron stripping followed by the



fragmentation of ${}^6\text{Li}$ into a deuteron and an alpha particle, or proton pickup followed by the breakup of ${}^8\text{Be}$ into two alpha particles.

Non-capture breakup can be unambiguously identified through the coincident measurement of the light emitted particles. Using this method, Martinez Heimann *et al.* have recently obtained integrated and differential cross sections of non-capture breakup reactions induced by the weakly bound ${}^6\text{Li}$ projectile on the spherical ${}^{144}\text{Sm}$ target [2]. Shrivastava *et al.* [3] conducted a detailed study of the transfer-breakup mechanism in the ${}^7\text{Li}+{}^{65}\text{Cu}$ system. In this case the observation of large cross sections for the $\alpha+d$ channel was interpreted as an evidence for a two-step process that consists in direct neutron transfer followed by the breakup of ${}^6\text{Li}$ via the 2.186 MeV resonance in the α -d continuum. Further evidence of this mechanism has shortly afterwards been found in the ${}^7\text{Li}+{}^{144}\text{Sm}$ system [4]. More recently, an extensive overview of these and other similar complex breakup modes in reactions of ${}^6\text{Li}$ and ${}^7\text{Li}$ projectiles on heavy targets has been presented in the work of Luong *et al.* [5].

On the other hand, the experimental identification and characterization of those breakup reactions that evolve towards the subsequent capture of one or both fragments (also called capture breakup) usually presents more ambiguities. This happens because in general the fragments originated in these processes may be similar to, and may have similar energies than, the residues produced in complete fusion reactions.

In this work we present the results of angular distribution measurements of the alpha particles emitted in the ${}^7\text{Li}+{}^{144}\text{Sm}$ system at energies around the Coulomb barrier. Lithium-7 presents an alpha cluster structure in its ground state and has a quite low energy threshold for the breakup into ${}^3\text{H}+{}^4\text{He}$ (2.45 MeV). Consequently, it is relatively easy to excite this mode in any nuclear collision, thus giving rise to relatively large cross-section for the production of alpha particles. We analyze and discuss the energy spectra and angular distributions of these particles by means of kinematical considerations related to the relevant mechanisms, and of the predictions of a statistical evaporation model. We place particular emphasis on the experimental procedure that we have used to unfold the contributions to the energy spectra originated not only in these processes, but also those coming from the target backing.

The study hereby reported is part of an ongoing effort by our research group that includes previous investigations of the ${}^{6,7}\text{Li}+{}^{144}\text{Sm}$ systems. For example, Figueira *et al.* [6] reported exhaustive measurements of elastic-scattering angular distributions from which reliable values of the optical potential parameters have been obtained. In particular, for the ${}^6\text{Li}+{}^{144}\text{Sm}$ system we have also carried out studies of breakup effects through measurements of inelastic scattering cross sections [7], of the alpha-particle production at extreme backward angles [8], and of the light particles emitted in coincidence as the result of non-capture breakup [2]. The analysis and interpretation of measurements of the α -d transfer-breakup mode in ${}^7\text{Li}+{}^{144}\text{Sm}$ is still underway and we expect to publish the results soon.

It is worth mentioning that other similar works as the one presented here have been done using weakly bound stable (e.g. Refs. [9, 10]) and radioactive (e.g. Refs. [11, 12]) projectiles over a range of target masses, energies and angles.

This article is organized as follows: The experimental procedure is detailed in Sect. 2. In Sect. 3 we describe the measurements, and discuss the preliminary results. Finally, in Sect. 4 we present the conclusions and outlook of this work.

2. Experimental procedure

The experiments were performed at the 20 UD TANDAR tandem accelerator in Buenos Aires, which delivered beams of ${}^7\text{Li}$ projectiles with bombarding energies of 18, 24 and 30 MeV. Typical beam currents ranged from 1 to 15 pA. The ${}^{144}\text{Sm}$ target was isotopically enriched to 96%, its thickness was $60\ \mu\text{g}/\text{cm}^2$, and it was evaporated onto a $20\text{-}\mu\text{g}/\text{cm}^2$ carbon backing.

The detection system used is a position-sensitive telescope for particle identification that consists of a segmented-anode ionization chamber filled with P10 gas, followed by an array of three silicon position-sensitive detectors (PSD). The angular acceptance of the whole device is 30° . For each

particle that impinged on the detector, the charge created by the energy loss along its path through the gas was collected by means of two successive anode segments. In this way, two partial energy loss signals ΔE_1 and ΔE_2 ($\Delta E = \Delta E_1 + \Delta E_2$) were produced. Finally, the particle was detected by one of the three PSDs, which allowed the determination of its residual energy E_{res} and its position of incidence. The energy resolution of the whole system was better than 3% (FWHM/centroid ratio), which was determined by a previous characterization using several ion beams at different energies and varying the ionization gas pressure of the chamber [13]. The angular uncertainty ranged from 0.2° to 0.3° , depending on the ionization gas pressure. No appreciable difference among the three PSDs in the energy resolution as well as in the angular straggling was observed. For a more detailed explanation of the employed technique see Ref. [13].

Figure 1 shows a bi-dimensional $E_{\text{res}}-\Delta E$ spectrum for the ${}^7\text{Li}+{}^{144}\text{Sm}$ system taken at $E_{\text{lab}} = 30$ MeV. In this case the E_{res} signals correspond to the central PSD that covers an angular range from 40° to 50° .

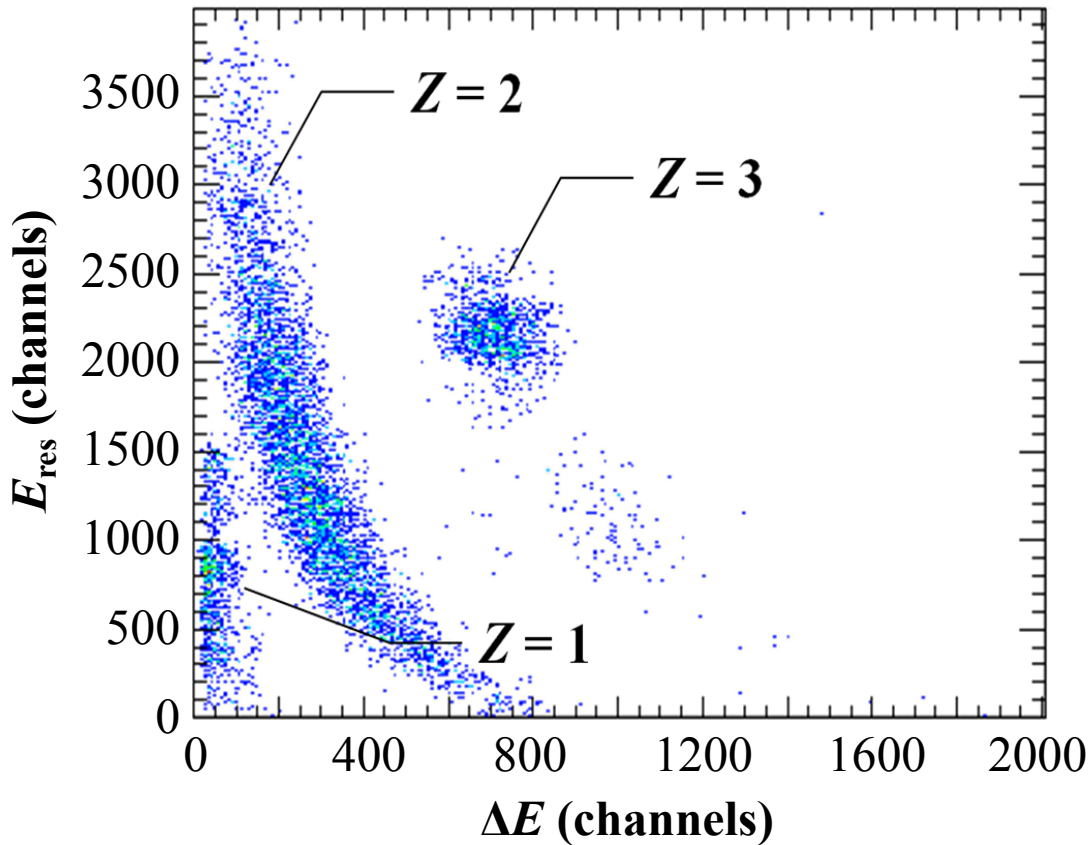


Figure 1. $E_{\text{res}}-\Delta E$ spectrum for the ${}^7\text{Li}+{}^{144}\text{Sm}$ system at $E_{\text{lab}} = 30$ MeV obtained with the central PSD placed at 45° .

In the data analysis procedure each PSD sensitive track was divided (by software) into bins of angular position. The effective solid angle Ω_{bin} subtended by each bin was determined using the elastic scattering of ${}^{16}\text{O}+{}^{197}\text{Au}$ at $E_{\text{lab}} = 50$ MeV. Thus, taking into account that at this energy the angular distribution of the elastically scattered ${}^7\text{Li}$ nuclei follows the Rutherford formula, the solid angle Ω_{bin} can be expressed as:

$$\Omega_{\text{bin}} = K \frac{N}{\delta} \left(\frac{d\sigma}{d\Omega}(\theta_{\text{bin}}) \right)^{-1} \quad (1)$$

where $d\sigma/d\Omega(\theta_{\text{bin}})$ is the differential cross section for Rutherford scattering for the $^{16}\text{O}+^{197}\text{Au}$ system at the bin angular position θ_{bin} , N is the number of ^7Li nuclei registered in the PSD bin, δ is the effective target thickness, and K is a normalization constant. The statistical error arising from N was less than 10% and the error in the thickness δ of the ^{197}Au target was estimated to be 10% by an independent measurement, being the latter the dominant contribution to the systematic uncertainty of the measured cross sections.

The measured angular range spanned from 15° to 140° . Since the detection system covers a range of 30° , four different angular positions of the ionization chamber were required in order to complete the whole distribution (15° - 45° , 45° - 75° , 75° - 105° , and 105° - 135°). At each position, an extra run was performed moving the detector by 5° in the backward direction to cover the dead zones between the PSDs.

The intensity of the ^7Li beam was determined by monitoring the elastically scattered particles on the ^{144}Sm target by means of a silicon surface barrier detector placed at a polar angle $\theta_{\text{mon}} = 28^\circ$, small enough to ensure pure Rutherford scattering for all the projectile energies.

The irradiation time of each run was such that the number of events in the $Z = 2$ group (see Fig. 1) was of the order of 3000 (2% statistical uncertainty). However, due to very small cross sections at backward angles, such requirement was relaxed to a few hundred events and/or the solid angle of the detection system was increased through a proper adjustment of the angular bins (see next Section).

3. Results and discussion

In Fig. 2 we present the alpha-particle energy spectra for the three projectile energies (18, 24 and 30 MeV) at three different angles ($\theta_{\text{bin}} = 20^\circ, 80^\circ$ and 140°). In all cases, the angle θ_{bin} corresponds to the center of a PSD bin for which an angular aperture $\Delta\theta_{\text{bin}} = 3^\circ$ was adopted by applying appropriate software cuts in the data analysis.

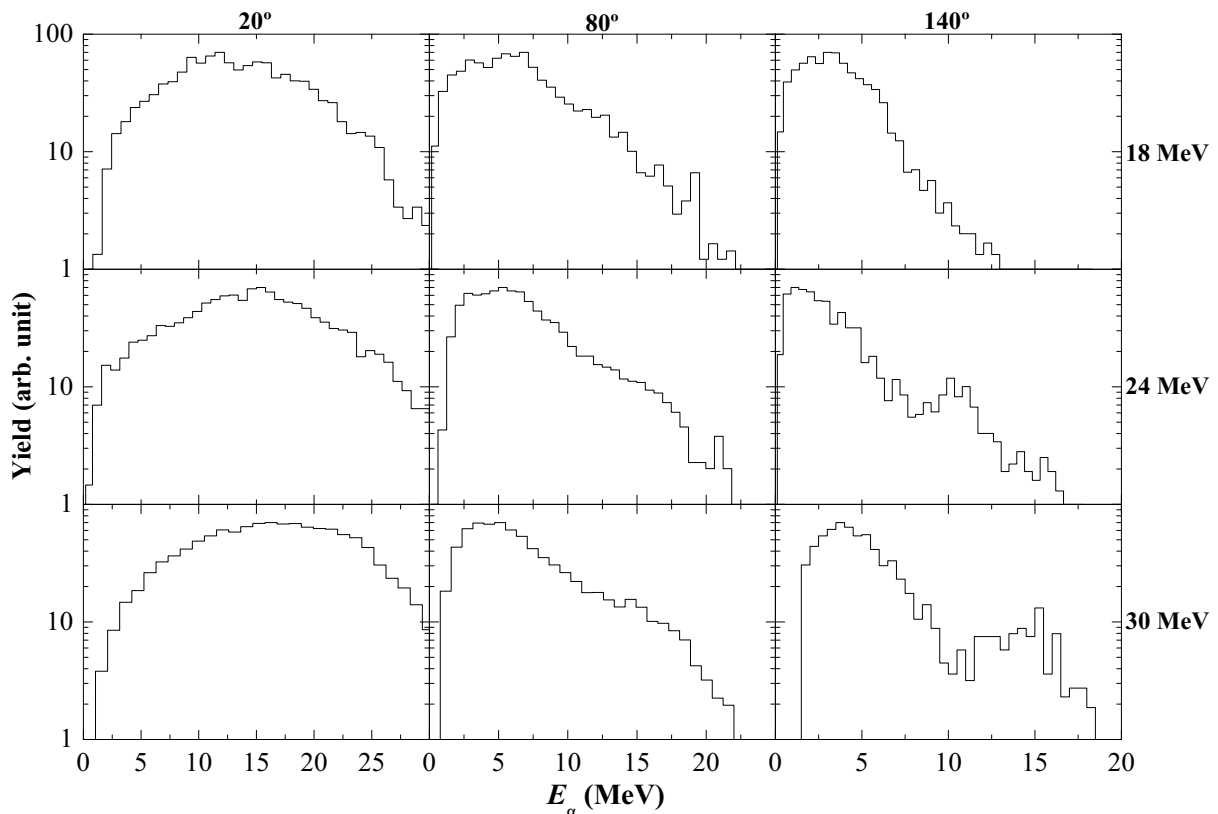


Figure 2. Energy spectra of the alpha particles emitted at $\theta_{\text{bin}} = 20^\circ, 80^\circ$ and 140° in the $^7\text{Li}+^{144}\text{Sm}$ system at $E_{\text{lab}} = 18, 24$ and 30 MeV. Each angle corresponds to the center of a $\Delta\theta_{\text{bin}} = 3^\circ$ PSD bin.

At the forward angles the spectra show no structure, but at more backward angles two groups of alpha particles with distinguishable energies appear. This feature is more evident at the highest bombarding energies (24 and 30 MeV) and at the most backward angle. The energy spectra obtained at 18 MeV seem to be structureless at all angles.

In the next Sub-section we will explore the different reactions that may explain the observed structures shown in Fig. 2.

3.1. Main sources of alpha particles

There are several possible two-, three- and four-body reactions that produce alpha particles for the weakly bound projectile ${}^7\text{Li}$. A list of these reactions with their respective ground-state Q -values is presented in Table 1.

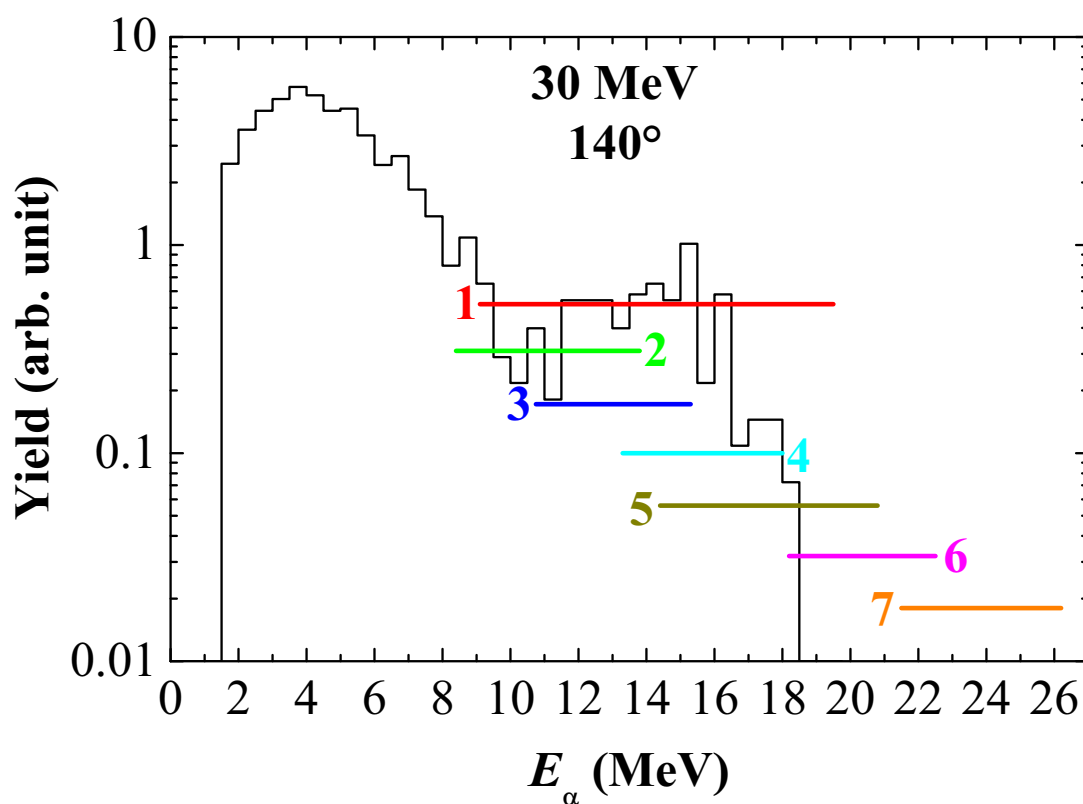


Figure 3. Energy spectrum of the alpha particles emitted in the ${}^7\text{Li}+{}^{144}\text{Sm}$ system at $E_{\text{lab}} = 30$ MeV and $\theta_{\text{bin}} = 140.0^\circ \pm 1.5^\circ$. The labeled segments indicate the expected energy ranges of the alpha particles that would be emitted in reactions listed in Table 1. The main group of events, at low energies has been identified as fusion between the ${}^7\text{Li}$ projectile and the ${}^{12}\text{C}$ from the target backing. See text for details.

Figure 3 shows an alpha-particle energy spectrum for ${}^7\text{Li}+{}^{144}\text{Sm}$ at $E_{\text{lab}} = 30$ MeV obtained with a PSD angular bin centered at $\theta_{\text{bin}} = 140.0^\circ \pm 1.5^\circ$. The labeled horizontal segments show typical energy ranges (the length represents the FWHM) of the alpha particles stemming from some of the processes listed in Table 1. For the case of incomplete fusion (channel 2 in Table 1), the mean energy has been estimated by imposing the simple model condition that the magnitudes of the asymptotic relative velocities are equal in the entrance channel (${}^7\text{Li}+{}^{144}\text{Sm}$) and in the exit channel ($\alpha+{}^{147}\text{Eu}$). The width has been obtained from a classical dynamical calculation using the code PLATYPUS [14]. Among the possible sources of alpha particles we have not considered the direct ${}^3\text{H}$ transfer to the low-lying excited states of ${}^{147}\text{Eu}$. In fact, the alpha particles emitted in such reactions have energies close to 34

MeV, well above the region of interest for the present study. For the processes that ultimately involve a binary breakup of the type $\alpha+X$ (channels 3 to 7 in Table 1) the corresponding energy distributions have been obtained with the code SUPERKIN [15]. For these cases, in the calculations we have taken into account the exact geometry of the detector as well as the dimensions of the bins used in the analysis, and we have assumed a representative uniform distribution of the center-of-mass relative energies between the breakup fragments (α and X) in the range 0 to 1 MeV. Using similar kinematical arguments, the mean energies of the alpha particles emitted in the four-body reactions (labeled 8 and 9 in Table 1, not shown in Fig. 3) have been estimated to be 14.0 MeV and 10.3 MeV, respectively.

Table 1. Reactions that produce alpha particles in the ${}^7\text{Li}+{}^{144}\text{Sm}$ system, with their respective ground state Q -values.

	Channel	Q -value (MeV)	
1	${}^{151}\text{Tb}^* \rightarrow \alpha + Y$	Complete fusion (CF)	4.56
2	$\alpha + {}^{147}\text{Eu}$	Incomplete fusion (ICF) / t-transfer	8.06
3	$\alpha + t + {}^{144}\text{Sm}$	Non-capture breakup (NCBU)	-2.47
4	$\alpha + d + {}^{145}\text{Sm}$	n-stripping followed by breakup	-1.97
5	$\alpha + \alpha + {}^{143}\text{Pm}$	p-pickup followed by breakup	11.05
6	$\alpha + n + {}^{146}\text{Eu}$	d-stripping followed by breakup	-0.44
7	$\alpha + p + {}^{146}\text{Sm}$	2n-stripping followed by breakup	4.22
8	$\alpha + n + n + {}^{145}\text{Eu}$	p-stripping followed by ternary breakup	-7.63
9	$\alpha + d + n + {}^{144}\text{Sm}$	Non-capture ternary breakup	-8.72

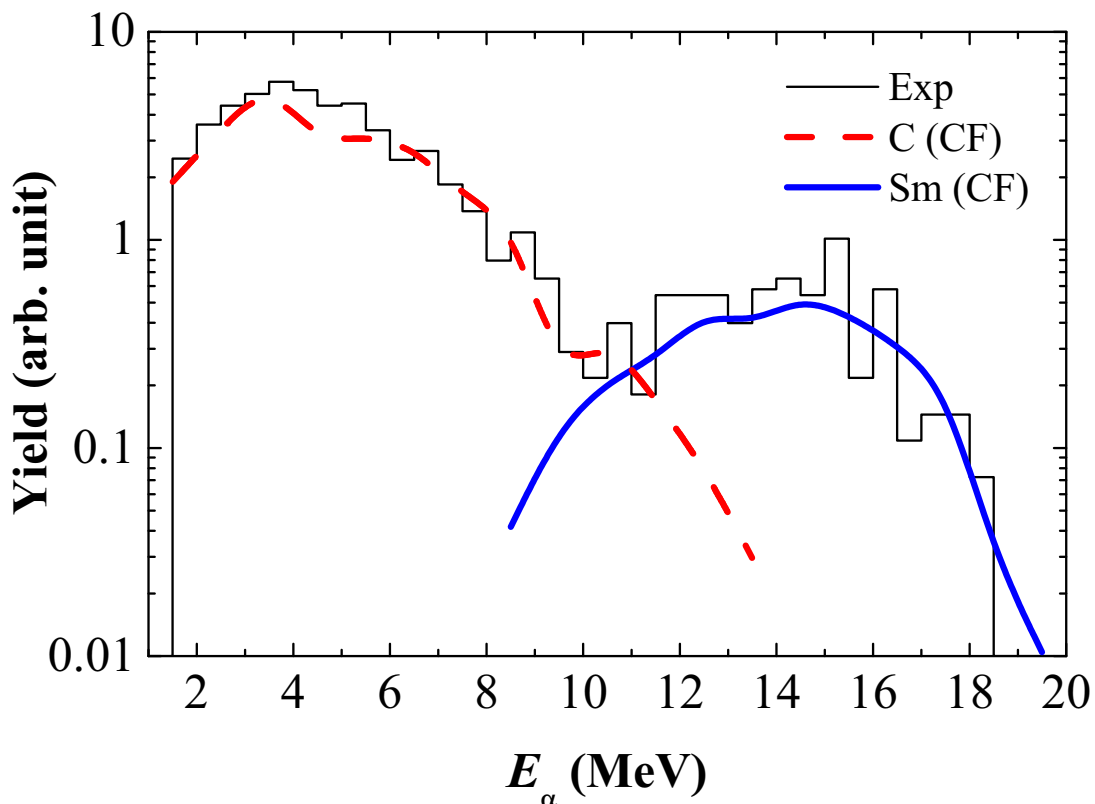


Figure 4. Alpha-particle energy spectrum for the ${}^7\text{Li}$ impinging on the ${}^{144}\text{Sm}$ target (and ${}^{12}\text{C}$ backing) at $E_{\text{lab}} = 30$ MeV and $\theta_{\text{bin}} = 140.0^\circ \pm 1.5^\circ$. The dashed and solid curves are theoretical calculations of complete fusion for the ${}^7\text{Li}+{}^{12}\text{C}$ and ${}^7\text{Li}+{}^{144}\text{Sm}$ systems, respectively.

From this kinematical analysis it is evident that all the reactions of interest existing in the ${}^7\text{Li}+{}^{144}\text{Sm}$ system produce alpha particles with higher energies than the main group of events in Fig. 3. It can be seen that the expected mean energies for capture and non-capture breakup happen to be in qualitative agreement with the high-energy bump observed in most energy spectra. Alpha particles coming from direct transfer reaction that would populate the ground states or the lowest excited states of the reaction products are expected to have much higher energies and they have not been observed in the present measurements. In general, based on all the possible reactions that involve only ${}^{144}\text{Sm}$, it is very difficult to find a quantitative explanation of the energy spectra over the whole energy range.

From these arguments we may conclude that the prominent low-energy bumps that are observed in all the spectra, most likely correspond to evaporation following the fusion of ${}^7\text{Li}$ projectiles with ${}^{12}\text{C}$ nuclei in the target backing. In order to further evaluate this hypothesis we have performed complete fusion-evaporation calculations for ${}^7\text{Li}+{}^{12}\text{C}$ (and ${}^7\text{Li}+{}^{144}\text{Sm}$) using the code PACE [16]. Figure 4 displays the same experimental spectrum as in Fig. 3 but now compared to the complete calculated energy distributions obtained with PACE. The excellent agreement of the calculation with the low-energy portion of the spectrum reinforces the above interpretation. In view of these results, for all the measured energy spectra we have decided to evaluate the high-energy tail of the alpha particles coming from ${}^7\text{Li}+{}^{12}\text{C}$ fusion and their contribution to the background over the region of interest for alpha particles coming from ${}^7\text{Li}+{}^{144}\text{Sm}$ reactions.

For this purpose we have resorted to auxiliary measurements with a pure ${}^{12}\text{C}$ target, which allowed us to parameterize the spectral shapes at different bombarding energies and emission angles using an asymmetric Gaussian function. In this way the ${}^{12}\text{C}$ fusion peak could be unequivocally determined in all the energy spectra and considered as background for the ${}^7\text{Li}+{}^{144}\text{Sm}$ data.

As an example of the procedure described above, in Fig. 5 we show background fits for ${}^7\text{Li}+{}^{144}\text{Sm}$ at $E_{\text{lab}} = 30$ MeV and at two different angles, $\theta_{\text{bin}} = 80^\circ$ and 140° . At this bombarding energy it was not possible to reliably separate the data of interest from the background below $\theta_{\text{lab}} \sim 80^\circ$. In the case of $E_{\text{lab}} = 24$ MeV, the angular limitation for a reliable separation of the alpha particles coming from reactions with ${}^{144}\text{Sm}$ from those originated in the backing was approximately $\theta_{\text{lab}} \geq 110^\circ$. Finally, at $E_{\text{lab}} = 18$ MeV the background subtraction procedure could not be satisfactorily applied at any angle. Therefore, we were unable to proceed with the angular distribution analysis at this lowest bombarding energy.

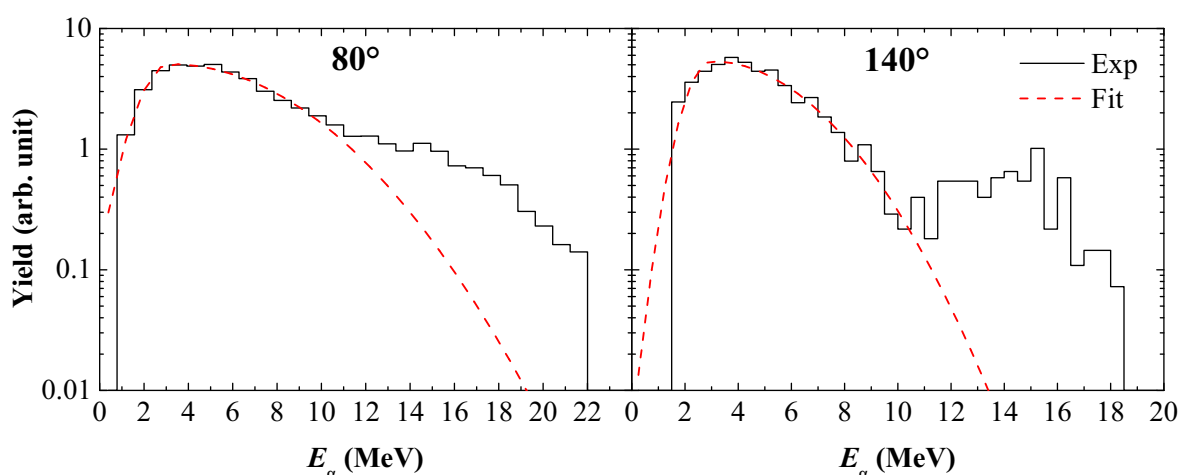


Figure 5. Fits of the ${}^7\text{Li}+{}^{12}\text{C}$ fusion background for $E_{\text{lab}} = 30$ MeV at two different angles: $\theta_{\text{bin}} = 80^\circ$ and 140° .

3.2. Angular distributions

Angular distributions of the emitted alpha particles have been obtained using the subset of data for which the previously described background-subtraction procedure could be reliably applied. Basically, this included data taken at $E_{\text{lab}} = 30$ MeV for $\theta_{\text{lab}} \geq 80^\circ$ and $E_{\text{lab}} = 24$ MeV for $\theta_{\text{lab}} \geq 110^\circ$. Within these angular ranges, the energy spectra were obtained for successive angular bins of constant width $\Delta\theta_{\text{bin}} = 3^\circ$ for both bombarding energies. By taking some measurements at overlapping angular positions of the detector, some of the angular gaps due to dead zones between adjacent PSDs could be filled out. After subtracting the background from each spectrum to obtain the alpha-particle yield that can be attributed to pure ${}^7\text{Li}+{}^{144}\text{Sm}$ reactions, the relative contribution of fusion-evaporation in comparison to the rest of the processes listed in Table 1 was evaluated. For that purpose we performed calculations with the code PACE, an example of which for $E_{\text{lab}} = 30$ MeV at $\theta_{\text{bin}} = 140^\circ$ is illustrated by the solid curve in Fig. 4. In this particular case (as well as in the rest of the data; not shown) we can observe that the calculation cannot account for the total alpha production over the energy region of interest. The yield of alpha particles in excess of the prediction can therefore be interpreted as arising from the sum of capture breakup and non-capture breakup processes.

The results of the present analysis are summarized in Fig. 6, where the differential cross sections for alpha-particle production as a function of laboratory scattering angles at $E_{\text{lab}} = 24$ and 30 MeV are shown. The empty and full circles represent the experimental total production whereas the dashed and solid curves correspond to the theoretical calculations of the corresponding fusion-evaporation contributions. In general, it can be observed that the contribution from fusion-evaporation cannot account for the measured cross sections of alpha-particle production. At 30 MeV the discrepancy is small at the most backward angles but it increases significantly as the emission angle decreases. At 24 MeV the contribution of fusion-evaporation to the total yield seems to be even less significant and it barely explains approximately one seventh of the experimental cross section.

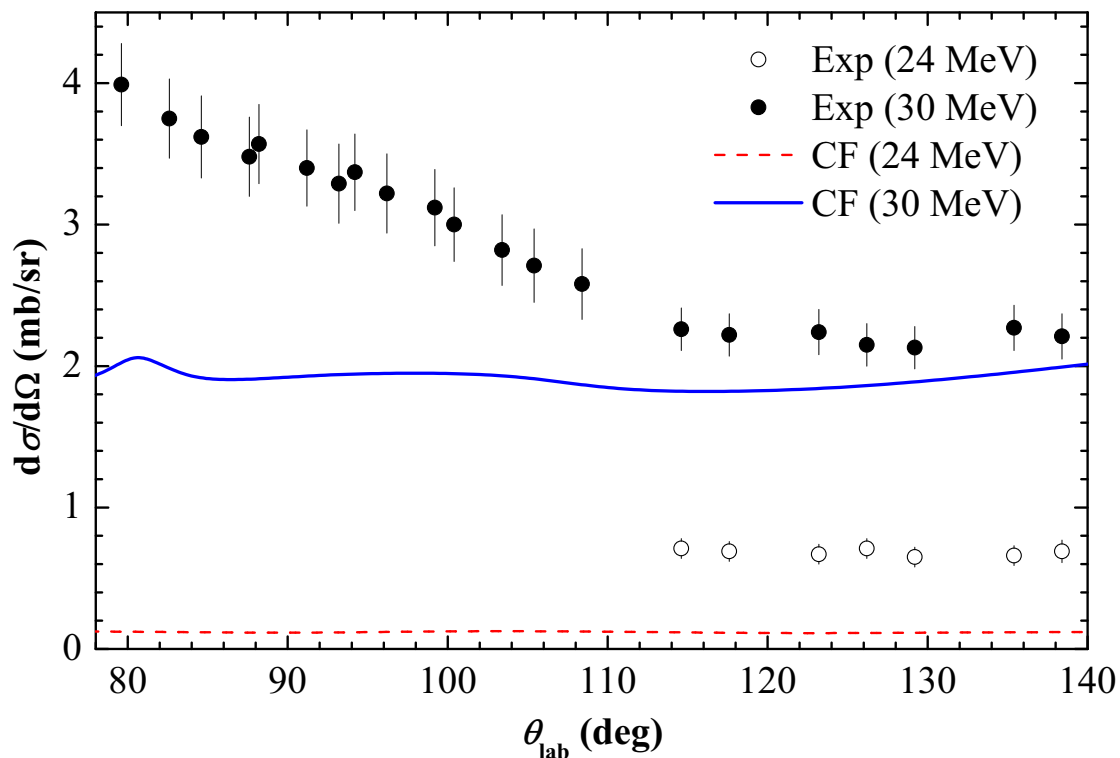


Figure 6. Angular distributions of the alpha-particle production cross section for the ${}^7\text{Li}+{}^{144}\text{Sm}$ system at laboratory energies of 24 and 30 MeV. Also shown are calculations of the corresponding fusion-evaporation contributions done with the code PACE.

Preliminary calculations based on the code PLATYPUS [14] showed us that the ICF and NCBU processes might account for these differences. The ICF has a rather uniform angular distribution in this range, but the NCBU is biased to forward angles. Hence the contribution of the NCBU process may explain the observed enhancement at angles around $\theta_{\text{lab}} \sim 80^\circ$ in the alpha angular distribution corresponding to $E_{\text{lab}} = 30$ MeV. An assessment of this hypothesis requires a better determination of the PLATYPUS input parameters that determine the breakup probability and the overall normalization factor for the ICF and NCBU processes. We are currently investigating this possibility.

4. Conclusions and outlook

We have measured the production of alpha particles using a ${}^7\text{Li}$ beam with bombarding energies of 18, 24 and 30 MeV on a ${}^{144}\text{Sm}$ target over a wide range of emission angles. The procedure that we have applied for the separation of the contribution from alpha particles produced in the carbon backing allowed us to obtain significant results only for $E_{\text{lab}} = 24$ and 30 MeV at backward angles ($\theta_{\text{lab}} > 80^\circ$). The sources of emission have been analyzed in the first place from a kinematical viewpoint, as a result of which we can establish a clear correspondence of the resulting energy spectra with fusion-evaporation and with capture (incomplete fusion) and non-capture breakup processes. No significant evidence was found of the most energetic alpha particles that would presumably originate in direct transfer reactions populating low-lying states of the transfer products. A further step in the analysis consisted in the estimate of the fusion-evaporation component by comparison with the results of calculations based on a statistical model. From the excess of the experimental cross sections over the predictions for fusion, we can evaluate the qualitative behavior of the combined breakup components as a function of bombarding energies and emission angles. At the highest measured bombarding energy (30 MeV) the results show an increasing contribution from breakup processes as we move to forward angles. At the lowest energy (24 MeV) breakup is clearly dominant over the whole measured angular range.

We are presently working on the last step of this analysis aimed to derive more quantitative information of the individual breakup components. Preliminary results obtained by application of a classical dynamical model appear to reproduce the order of magnitude of the measured cross sections and the qualitative angular dependence of the alpha-particle emission originated in breakup reactions. We expect to be able to improve the analysis from both the experimental and theoretical sides. Regarding the calculations, we are investigating the use of more reliable input parameters of the model, such as the breakup probabilities that can be obtained from a systematic evaluation of previous experiments. We are planning to incorporate the results of our recent exclusive cross-section measurements of the transfer-breakup mechanism, consisting in the coincident detection of deuterons and alpha particles in reactions induced by ${}^7\text{Li}$ projectiles. We also intend to apply the whole procedure described in this work to the study of other reaction systems such as ${}^7\text{Li}+{}^{27}\text{Al}$ system, which has already been measured and which analysis is currently underway.

References

- [1] Canto L F, Gomes P R S, Donangelo R and Hussein M S 2006 *Phys. Rep.* **424** 1
- [2] Martinez Heimann D, Pacheco A J, Capurro O A, Arazi A, Balpardo C, Cardona M A, Carnelli P F F, De Barbará E, Fernández Niello J O, Figueira J M, Hojman D L, Martí G V, Negri A E and Rodrigues Ferreira Maltez D 2014 *Phys. Rev. C* **89** 014615
- [3] Shrivastava A, Navin A, Keeley N, Mahata K, Ramachandran K, Nanal V, Parkar V V, Chatterjee A and Kailas S 2006 *Phys. Lett. B* **633** 463
- [4] Martinez Heimann D, Pacheco A J, Arazi A, Capurro O A, Carnelli P F F, Monteiro D S, Fernández Niello J O, Figueira J M, Fimiani L, Grinberg P, Marta H D, Martí G V, Negri A E and Testoni J E 2009 *AIP Conf. Proc.* **1098** 275
- [5] Luong D H, Dasgupta M, Hinde D J, Du Rietz R, Rafiei R, Lin C J, Evers M and Diaz-Torres A 2011 *Phys. Lett. B* **695** 105
- [6] Figueira J M, Fernández Niello J O, Arazi A, Capurro O A, Carnelli P F F, Fimiani L, Martí G

- V, Martinez Heimann D, Negri A E, Pacheco A J, Lubian J, Monteiro D S and Gomes P R S 2010 *Phys. Rev. C* **81** 024613
- [7] Woodard A E, Figueira J M, Otomar D R, Fernández Niello J O, Lubian J, Arazi A, Capurro O A, Carnelli P F F, Fimiani L, Martí G V, Martinez Heimann D, Monteiro D S, Negri A E, Pacheco A J and Gomes P R S 2012 *Nucl. Phys. A* **873** 17
- [8] Capurro O A, Pacheco A J, Arazi A, Figueira J M, Martinez Heimann D and Negri A E 2011 *Nucl. Phys. A* **849** 1
- [9] Kelly G R, Davis N J, Ward R P, Fulton B R, Tungate G, Keeley N, Rusek K, Bartosz E E, Cathers P D, Caussyn D D, Drummer T L and Kemper K W 2000 *Phys. Rev. C* **63** 024601
- [10] Signorini C, Edifizi A, Mazzocco M, Lunardon M, Fabris D, Vitturi A, Scopel P, Soramel F, Stroe L, Prete G, Fioretto E, Cinausero M, Trotta M et al. 2003 *Phys. Rev. C* **67** 044607
- [11] Kolata J J, Goldberg V Z, Lamm L O, Marino M G, O’Keeffe C J, Rogachev G, Aguilera E F, García-Martínez H, Martínez-Quiroz E, Rosales P et al. 2002 *Phys. Rev. C* **65** 054616
- [12] De Faria P N, Lichtenthäler R, Pires K C C, Moro A M, Lépine-Szily A, Guimarães V, Mendes D R Jr, Arazi A, Barioni A, Morcelle V and Morais M C 2010 *Phys. Rev. C* **82** 034602
- [13] Carnelli P F F, Arazi A, Fernández Niello J O, Capurro O A, Cardona M A, De Barbará E, Figueira J M, Hojman D L, Martí G V, Martinez Heimann D, Negri A E and Pacheco A J 2013 *Nucl. Inst. and Meth. A* **726** 116
- [14] Diaz-Torres A 2010 *J. Phys. G* **37** 075109
- [15] Martinez Heimann D, Pacheco A J and Capurro O A 2010 *Nucl. Inst. and Meth. A* **622** 642
Martinez Heimann D, Pacheco A J and Capurro O A 2012 *Nucl. Inst. and Meth. A* **694** 313
- [16] Gavron A 1980 *Phys. Rev. C* **21** 230